

1, 1992, pp. 1–34.

⁷Zang, T. A., Dahlburg, R. B., and Dahlburg, J. P., "Direct and Large Eddy Simulations of Three-Dimensional Compressible Turbulence," *Physics of Fluids A*, Vol. 4, No. 1, 1992, pp. 127–140.

⁸Shebalin, J. V., and Montgomery, D., "Turbulent Magnetohydrodynamic Density Fluctuations," *Journal of Plasma Physics*, Vol. 39, No. 2, 1988, pp. 339–367.

⁹Zeman, O., "Progress in Modeling Hypersonic Turbulent Boundary Layers," *Annual Research Briefs–1992*, Center for Turbulence Research, NASA Ames Research Center, Moffett Field, CA, Jan. 1993, pp. 213–225.

¹⁰Vincenti, W. G., and Kruger, C. H., *Introduction to Physical Gas Dynamics*, Wiley, New York, 1965, pp. 407–412.

¹¹Shebalin, J. V., "Pseudospectral Simulation of Compressible Turbulence Using Logarithmic Variables," AIAA 11th Computational Fluid Dynamics Conference, AIAA Paper 93-3375, Orlando, FL, July 1993.

¹²Abarbanel, S., Dutt, P., and Gottlieb, D., "Splitting Methods for Low Mach Number Euler and Navier-Stokes Equations," *Computers & Fluids*, Vol. 17, No. 1, 1989, pp. 1–12.

¹³Thompson, P. A., *Compressible-Fluid Dynamics*, McGraw-Hill, New York, 1972, p. 30.

¹⁴Canuto, C., Hussaini, M. Y., Quateroni, A., and Zang, T. A., *Spectral Methods in Fluid Dynamics*, Springer-Verlag, New York, 1988, p. 83, pp. 255–273.

¹⁵Gazdag, J., "Time-Differencing Schemes and Transform Methods," *Journal of Computational Physics*, Vol. 20, No. 2, 1976, pp. 196–207.

¹⁶Gilbarg, D., and Paolucci, D., "The Structure of Shock Waves in the Continuum Theory of Fluids," *Journal for Rational Mechanics and Analysis*, Vol. 2, No. 4, 1953, pp. 617–642.

¹⁷Landau, L. D., and Lifshitz, E. M., *Fluid Mechanics*, 2nd ed., Pergamon, Oxford, England, UK, 1987, p. 335.

¹⁸Shebalin, J. V., "Aerobreaker Plasmadynamics: Macroscopic Effects," *Journal of Spacecraft and Rockets*, Vol. 28, No. 4, 1991, pp. 394–400.

¹⁹Ribner, H. S., "Spectra of Noise and Amplified Turbulence Emanating from Shock-Turbulence Interaction," *AIAA Journal*, Vol. 25, No. 3, 1987, pp. 436–442.

²⁰Lee, S., Lele, S. K., and Moin, P., "Direct Numerical Simulation of Shock Turbulence Interaction," AIAA Paper 91-0523, Jan. 1991.

²¹Hannappel, R., and Friedrich, R., "Interaction of Isotropic Turbulence with a Normal Shock Wave," *Applied Scientific Research*, Vol. 51, No. 2, 1993, pp. 507–512.

²²Richtmeyer, R. D., and Morton, K. W., *Difference Methods for Initial Value Problems*, 2nd ed., Interscience, New York, 1967, p. 312.

Generalized Vortex Lattice Method for Oscillating Thin Airfoil in Subsonic Flow

Paulo A. O. Soviero*

Instituto Tecnológico de Aeronáutica,
12228-900 São José dos Campos, S.P., Brazil

Nomenclature

h	= nondimensional vertical displacement amplitude
J_0	= Bessel's function of first kind and zero order
K	= $krM/(1 - M^2)$
kr	= reduced frequency
M	= undisturbed flow Mach number
Y_0	= Bessel's function of second kind and zero order
β	= $(1 - M^2)^{1/2}$
$\delta\phi$	= perturbation velocity potential jump across airfoil and wake
πk	= complex lift coefficient for unitary amplitude
$\pi m/2$	= complex pitch moment coefficient, about midchord, for unitary amplitude

Superscripts

'	= real part of k and m
"	= imaginary part of k and m

Subscripts

a	= relative to heaving motion
b	= relative to pitching motion

Introduction

DESPITE the wide attention paid to the important problem of a harmonically oscillating thin airfoil in a subsonic flow,^{1,2} the panel method approach,³ or even its simplest variant, namely, the vortex lattice method, has been used only recently for the problem solution. The reason for this may be attributed to the fact that, when solving the problem for the velocity potential, the wake must explicitly be taken in account. Another reason may be the already wide accumulation of knowledge of singular kernels which occurs when acceleration potential formulations are made, as in Possio's integral equation.²

Except for approximated solutions,⁴ it appears that numerical methods are the only tools which may be employed to solve the high frequency and Mach number cases without significant losses in precision and in a sufficiently general way.

In the present work, the generalized vortex lattice method⁵ is applied to the two-dimensional case of harmonically oscillating flat plate in a subsonic flow. Two modes of motion have been considered, namely, the pitching and heaving modes.

The reasons the present method is called a generalized vortex lattice will be presented, qualitatively, in the next section. For a complete discussion about the method the reader is referred to Ref. 5.

Mathematical Model and Its Integral Equation

A two-dimensional flat plate in small pitching and heaving harmonic motion is considered in an otherwise steady subsonic flow which streams along the positive X -axis direction.

The undisturbed flow velocity and reference length (semi-chord) are made unitary. In this case the linearized equation and boundary conditions for the perturbation velocity potential can be reduced to the following system of equations^{5,6}:

$$\frac{\partial^2 \phi}{\partial X^2} + \frac{\partial^2 \phi}{\partial Z^2} + K^2 \phi = 0 \quad (1)$$

$$\frac{\partial \phi}{\partial Z} = \exp(-iKMX) / \beta \left(\frac{\partial h}{\partial X} + ikrh \right) \quad -1 \leq X \leq 1 \quad (2a)$$

$$\frac{iK}{M} \delta\phi + \frac{\partial \delta\phi}{\partial X} = 0, \quad X \geq 1 \quad (2b)$$

Equation (2a) is applied on flat plate surface and Eq. (2b) over the wake.

Solving Eq. (1) for ϕ , the nondimensional pressure coefficient for profile and wake is obtained from

$$C_p = -2 \exp(iKMX) \left(\frac{iK}{M} \phi + \frac{\partial \phi}{\partial X} \right) \quad (3)$$

It is worthwhile to note that Eq. (2b) results from the application of Eq. (3) to both sides of the wake and then imposing pressure continuity. At the trailing edge, $X = 1$, Eq. (2b) also assures the Kutta condition.

The integral equation that relates the velocity potential jump across the flat plate and wake to the velocity potential in an arbitrary field point can be expressed as⁷

$$\phi_P = -\frac{1}{4} \int_{-1}^{\infty} \delta\phi \frac{\partial}{\partial n} [D_0(KR)] dX \quad (4)$$

The elementary solution of the Helmholtz two-dimensional Eq. (1) can be written as⁷

$$D_0(KR) = -Y_0(KR) - iJ_0(KR) \quad (5)$$

and is the two-dimensional point source of four units intensity.

The velocity component normal to the profile surface is obtained by taking the Z derivative of Eq. (5) which reads as

$$\frac{\partial \phi_P}{\partial Z} = -\frac{1}{4} \int_{-1}^{\infty} \delta \phi \frac{\partial^2}{\partial Z \partial n} [D_0(KR)] dX \quad (6)$$

The mathematical problem solution has been obtained by solving Eq. (6) numerically subjected to boundary conditions [Eqs. (2a) and (2b)] for the profile and wake, respectively.

The resulting equation allows a physical interpretation along the same lines as in the incompressible case. In fact, it can be stated that the integrand represents a normal doublet density $\delta \phi$, distributed over a line element dX . If, in the discretization procedure, $\delta \phi$ is made constant over each element, the well-known vortex lattice method for incompressible flow is recovered, simply by making K tend to zero. Then, the two-dimensional point vortex formulation is recovered, which is, in fact, composed of infinitely long line vortices.

Numerical Solution and Results

Consider a flat plate lying in the X axis and divided in NX panels. A wake of finite length, sufficiently long to assure convergence, is also modeled by an uniform mesh of NE equally spaced panels.

Over each panel the velocity potential jump $\delta \phi$ is taken as constant. The numerical scheme that results from discretization of Eq. (6) and boundary conditions [Eqs. (2a) and (2b)] corresponds formally to the same system of linear complex equations presented in Ref. 5. The complex influence coefficients are calculated numerically from Eq. (6) simply by making $\delta \phi = 1$.

To obtain the complex influence coefficient of a panel in its own control point, the definition of the normal velocity is obtained as the limit as given in Ref. 8.

The numerical calculations using the present method have been performed for a flat plate oscillating in pitch around an axis through the leading edge. The real part of the pressure coefficient difference distributed along the chord is compared

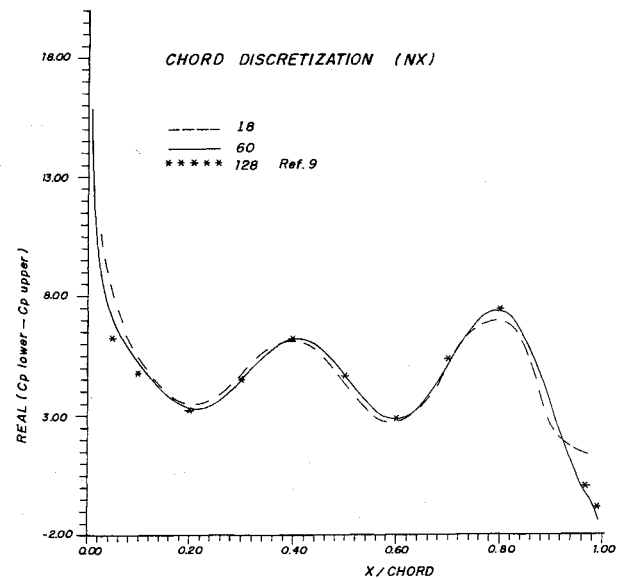


Fig. 1 Two-dimensional real pressure coefficient difference along the profile pitching around the leading-edge axis: $M = 0.9$ and $kr = 0.9.s$

in Fig. 1 to results of Ref. 9. In the present work the wake is five chords long. Both cases with low panel density ($NX = 18$) and high panel density ($NX = 60$) discretizations compare favorably with the reference case⁹ ($NX = 128$).

In a second series of calculations force and pitching moment coefficients are calculated for several Mach numbers and reduced frequencies for the flat plate in pitching and heaving motions about an axis through the midchord. The results are compared with Ref. 10.

For a profile discretization of $NX = 60$ and a five-chord long wake, the numerical results of pure heaving and pure pitching motions aerodynamic coefficients are displayed in Tables 1 and 2, respectively. For each Mach number case the first row corresponds to present method calculations and the second row to data of Ref. 10.

Except for the value of k_b'' for $M = 0.6$ and $kr = 3.2$, see Table 2, the overall agreement is quite good.

Concluding Remarks

Similarly to the three-dimensional case of Ref. 5, in the present work the well-known concepts of point vortices and doublets have been extended to the compressible oscillatory range. From the elementary solution of the Helmholtz equation all of the conclusions obtained in Ref. 5 may be easily adapted to the two-dimensional case. In fact, the incompressible equivalence between a vortex pair and a line of constant density potential must be, in the present work, complemented in the compressible regime by a line integral which is proportional to the square of K .

References

- Timman, R., van de Vooren, A. I., and Greidanus, J. H., "Aerodynamic Coefficients of an Oscillating Airfoil in Two-Dimensional Subsonic Flow," *Journal of the Aeronautical Sciences*, Vol. 18, Dec. 1951, pp. 797-802.
- Kemp, N. H., and Homicz, G., "Approximate Unsteady Thin-Airfoil Theory for Subsonic Flow," *AIAA Journal*, Vol. 14, No. 8, 1976, pp. 1083-1089.
- Leong, S. H., "A Panel Method Computation for Oscillating Aerofoil in Compressible Flow," *International Journal for Numerical Methods in Engineering*, Vol. 29, No. 3, 1990, pp. 559-578.
- Amiet, R. K., "High Frequency Thin-Airfoil Theory for Subsonic Flow," *AIAA Journal*, Vol. 14, No. 8, 1976, pp. 1076-1082.
- Soviero, P. A. O., and Bortolus, M. V., "A Generalized Vortex Lattice Method for Oscillating Lifting Surfaces in Subsonic Flow," *AIAA Journal*, Vol. 30, No. 11, 1992, pp. 2723-2729.
- Bisplinghoff, R. L., Ashley, H., and Halfman, R. L., *Aeroelasticity*, Addison-Wesley, Reading, MA, 1955, pp. 326-328.

Table 1 Force and moment coefficients: heaving motion

M	kr	k_a'	k_a''	m_a'	m_a''
0.8	1.8	0.33333 ^a	-2.50829	-0.43601	0.09499
		0.31751 ^b	-2.51642	-0.43858	0.09528
0.7	1.74857	0.50159 ^a	-2.64306	-0.54739	0.06449
		0.49529 ^b	-2.64753	-0.54909	0.06614
0.6	3.2	1.42659 ^a	-6.68763	-0.66090	0.47682
		1.39471 ^b	-6.71096	-0.66588	0.47911
0.6	1.70667	0.61302 ^a	-3.05761	-0.92802	-0.09273
		0.60559 ^b	-3.05676	-0.92567	-0.08932

^aPresent method. ^bFrom Ref. 10.

Table 2 Force and moment coefficients: pitching motion around the midchord axis

M	kr	k_b'	k_b''	m_b'	m_b''
0.8	1.8	1.83884 ^a	0.07488	-0.20107	-0.97268
		1.83661 ^b	0.08111	-0.20169	-0.97367
0.7	1.74857	2.06636 ^a	0.20332	-0.17118	-1.12716
		2.06328 ^b	0.21709	-0.16975	-1.12835
0.6	3.2	2.77411 ^a	-0.08085	0.14516	-1.68166
		2.76302 ^b	-0.04326	0.14946	-1.68445
0.6	1.70667	2.72006 ^a	0.42901	0.15509	-1.55038
		2.71678 ^b	0.44410	0.15748	-1.55086

^aPresent method. ^bFrom Ref. 10.

⁷Lamb, H., *Hydrodynamics*, 6th ed., Cambridge University Press, Cambridge, England, UK, 1975, p. 531.

⁸Bousquet, J., *Methode des Singularites*, Cepadues-Editions, Toulouse, France, 1990, pp. 148-157.

⁹Rowe, W. S., "Comparison of Analysis Methods Used in Lifting Surface Theory," *Computational Methods in Potential Aerodynamics*, Springer-Verlag, Berlin, Germany, 1985, pp. 198-239.

¹⁰Anon., "Tables of Aerodynamic Coefficients for an Oscillating Wing-Flap System in a Subsonic Compressible Flow," Nationaal Luchtvaartlaboratorium, Rept. F 151, Amsterdam, The Netherlands, May 1954.

Disperse Phase Motion in Neutrally Buoyant and Zero-Gravity Pipe Flows

K. R. Sridhar*

University of Arizona, Tucson, Arizona 85721
and

B. T. Chao†

University of Illinois at Urbana-Champaign,
Urbana, Illinois 61801

Introduction

It has been shown by Sridhar et al.¹ that the dynamics of steady, fully developed, turbulent, dispersed liquid-vapor duct flows in zero gravity can be simulated by using two immiscible, neutrally buoyant liquids in an Earth-based flow facility. Such simulation experiments have been used to predict the frictional pressure drop in a zero-gravity environment. Theoretical analysis showed that the mean discrete-phase velocity and the local mean continuous-phase velocity are identical in liquid-vapor flow in zero gravity and in liquid-liquid flows of neutral buoyancy on Earth. This finding forms the cornerstone of the simulation scheme. However, only a limited amount of experimental data supporting this finding was reported.¹

The equation of motion for a Stokesian sphere in unsteady, nonuniform flow was rigorously derived by Maxey and Riley.² The equation for the dispersed phase used in the analysis of Sridhar et al.¹ was based on the equation due to Maxey and Riley and modified to account for a multiparticle system and non-Stokesian motion. The modification was not rigorous. The equation for the continuous phase was formulated by subtracting the dispersed phase equation from the momentum equation for the mixture. The results show that the mean continuous phase velocity U_c is equal to the mean discrete-phase velocity U_d , for both 0-g liquid-vapor flows and 1-g neutrally buoyant flows. Because of the fundamental nature of this result, and its importance to microgravity simulation, additional experiments were conducted for its validation.

Related Work

Batchelor et al.³ made extensive measurements of the mean velocity of single, neutrally buoyant particles in fully developed turbulent pipe flow of water and related the mean velocity to the discharge velocity. They were interested in comparing the Lagrangian average of the velocity of a material element of the fluid with the Eulerian average of the fluid velocity at fixed points. The particle velocity was measured

using photographic detectors and timing slits provided along the length of the pipe. The discharge velocity was determined with a measuring tank.

To relate the velocity of a particle to that of the fluid, Batchelor et al.³ assumed that the mean particle velocity is equal to the mean velocity of the undisturbed fluid at the same location as the center of the particle, provided that the particle is so small that the mean fluid velocity does not vary appreciably over a distance equal to the particle diameter. For larger particles, they took the mean particle velocity as equal to the fluid velocity averaged over the cross section of the particle. Furthermore, it was recognized that the material element in turbulent pipe flow wandered freely over any region of a cross section and a particle of finite size would not have the same freedom. If the pipe radius is r_0 and the particle is a sphere of radius αr_0 , the center of the particle is free to move down the pipe only within a cylinder of radius $(1 - \alpha)r_0$. Thus, the probability of finding the center of the particle inside the cylinder is the same for all positions and is zero outside the cylinder. The results of their experiments confirmed the theoretical prediction that the local discharge velocity, the ensemble average of the velocity of a material element, and the velocity of a material element averaged over a long time are all equal. The Lagrangian average of the velocity of a material element was determined by spheres of various sizes and extrapolated to zero size. Thus, a corollary of the investigation by Batchelor et al. is that the mean velocity of the neutrally buoyant spheres in turbulent pipe flow is identical to the mean velocity of the undisturbed fluid at the same location. The latter is to be determined by averaging over the cross section of the sphere. The experiments of Batchelor et al. were for single particles. The purpose of this Note is to demonstrate that the conclusion $U_c = U_d$ remains valid for multiparticle systems.

Experimental Facility

The two neutrally buoyant immiscible liquids used in the experiments were water for the continuous phase and n-butyl benzoate ($C_6H_5COOC_4H_9$) for the dispersed phase (droplets). Two series of experiments were conducted, one with a square test section and another with a circular test section. The square test section had an inside dimension of 50.8 mm on a side and a length of 1.83 m. The circular test section was made by connecting together four 15.4-mm i.d. Pyrex glass tubes, each 1.22 m long. A globe valve located downstream of a centrifugal pump was used to control the flow rate of water through the test section, and monitoring was done using a venturi and a Validyne differential pressure transducer. The velocity of the droplets was measured using particle image velocimetry. The underlying principle behind this technique is to mark time and record the spatial displacements of the droplets. This was achieved by means of an EG&G Type 501 stroboscope and a 35-mm still camera. Details of the setup, instrumentation, and experimental procedure can be found in Sridhar et al.¹

Results and Discussion

In the first series of experiments, water was pumped through the 50.8-mm square test section at a rate of $1.274 \times 10^{-3} \text{ m}^3 \text{ s}^{-1}$ and benzoate was injected into the flow at a rate of $8.83 \times 10^{-6} \text{ m}^3 \text{ s}^{-1}$, giving rise to a range of drop sizes. The area-averaged mixture velocity was 0.497 m s^{-1} , and the flow Reynolds number was 25,200. The stroboscope was flashed at a frequency of 50 Hz, and the shutter of the still camera was open for a duration of 0.4 s. Only droplets in the central one-third of the square cross section, where the water velocity profile was relatively flat, were used. The photographs revealed that the droplets were spherical and almost completely free from distortion. Data were gathered for a total of 48 droplets in the fully developed region with diameters ranging from less than 2 to 5 mm. The results of the average velocities for the four size groups and their standard deviations have already been reported.¹ It was shown that the drop velocities are independent of their sizes, and their variation among the groups is within experimental error. It was also shown that the average water

Received Dec. 15, 1992; revision received March 16, 1993; accepted for publication March 19, 1993. Copyright © 1993 by the American Institute of Aeronautics and Astronautics, Inc. All rights reserved.

*Assistant Professor, Department of Aerospace and Mechanical Engineering, Member AIAA.

†Professor Emeritus, Department of Mechanical and Industrial Engineering, 1206 W. Green Street.